JOURNAL OF MATERIALS SCIENCE **33** (1998) 5901–5904

Apatite–wollastonite glass-ceramics

Part I *Crystallization kinetics by differential thermal analysis*

S. LIKITVANICHKUL, W. C. LACOURSE
New York State College of Ceramics at Alfred University, Alfred, NY 14802, USA
E-mail: sumalee@mtec.or.th

Apatite crystallization in the apatite–wollastonite glass exhibits a three-dimensional bulk mechanism with an Avrami parameter (n) ≈ 3, while that of the second phase (wollastonite) shows a two-dimensional surface mechanism (planar growth) with $n \approx 2$. A strong effect of glass particle size on the wollastonite crystallization temperature is observed. The peak temperature is lower when the particle size is smaller.

1. Introduction

Bioactive apatite–wollastonite (A–W) glass-ceramics exhibit high fracture toughness and strength, which allow them to be used as load-bearing implants [1, 2]. Formation of a wollastonite phase upon appropriate heat treatment is responsible for the substantial increase in mechanical properties [2, 3]. However, crystallization of the wollastonite phase creates defects, such as pores, cracks, etc., and, in the worst case, even breaks a bulk sample. Such behaviour limits the bulk-glass forming method for this composite material. Recently, this material has been manufactured by ceramic powder processing technique, i.e. pulverizing the glass, compacting the glass powders, and ceramming to form a glass-ceramic [4, 5].

Details on crystallization kinetics of this glass system have not been published. The crystallization kinetic parameters found by differential thermal analysis (DTA) indicate that crystallization of the apatite phase is a three-dimensional bulk process and that of the wollastonite phase is a two-dimensional planar growth, surface process. The DTA studies show the strong effect of glass particle size on the crystallization temperature of the wollastonite phase.

2. Experimental procedure

Glasses were prepared from reagent grade $CaCO_3$, SiO_2, MgO, $CaHPO_4{\cdot}2H_2O$, and CaF_2. Composition of glasses melted here was based on information from Nakamura [1], provided in Table I. Batches were melted in covered platinum–10% rhodium crucibles for 2 h in an electric furnace at 1450 °C. Glasses were cast in heated graphite moulds.

Glass transition temperatures, T_g, were determined by a horizontal dual pushrod dilatometer (Innovative Thermal System, Atlanta, GA). The measurement was made at a heating rate of 3 K min^{-1}, using sapphire as a reference. The T_g's were evaluated using the tangent intersection method.

Glasses were crushed and sieved through a series of screens. Particle sizes in the range of 1–2 mm to $<45\ \mu$m were prepared. They were stored in an oven maintained at $\approx$120 °C until used for the differential thermal analysis (DTA) measurements. Runs were made on 90 ± 0.1 mg samples in a platinum crucible. The accuracy of the instrument was verified using silver standards. Particles with sizes of 1–2 mm (coarse) and 180–250 μm (fine) were used for the crystallization kinetic studies. The measurements were performed at a heating rate of 5, 7, 10, and 15 K min^{-1} in a flowing nitrogen atmosphere. The data were analysed using the Kissinger equation [6]

$$\ln\left(\frac{\phi}{T_P^2}\right) = -\frac{E}{RT_P} + C \tag{1}$$

where ϕ is the heating rate, R is the gas constant, T_P is the crystallization peak temperature, E is the activation energy for crystallization, and C is a constant. The activation energy was determined from a plot of $\ln(\phi/T_P^2)$ versus $1000/T_P$.

The Avrami parameter, n, can be calculated from a single exotherm using the equation presented by Augis and Bennett [7]

$$n = \frac{2.5RT_P^2}{\mathrm{FWHM}\ E} \tag{2}$$

The Avrami parameter can be used to indicate shape and dimensionality of the crystal growth, i.e. $n = 1$ for 1-D, $n = 2$ for planar (both denote surface crystallization), and $n = 3$ for three-dimensional bulk crystallization [8–10].

The effect of glass particle size on crystallization of the A–W glass was studied using glass with particle sizes shown in Table II. The measurements were made at a heating rate of 5 K min^{-1} in a flowing nitrogen atmosphere to a maximum temperature of 1100 °C.

TABLE I Batch composition

	MgO	CaO	SiO_2	P_2O_5	CaF_2
Wt %	4.6	44.7	34.0	16.2	0.5
Mol %	7.1	49.9	35.5	7.1	0.4

TABLE II Glass particle size

Range of particle size	
(mesh)	(mm or μm)
−10+16	1–2 mm
−20+35	425–850 μm
−35+45	325–425 μm
−60+80	180–250 μm
−80+120	120–180 μm
−120+170	90–120 μm
−325	<45 μm

3. Results and discussion

The glass transition temperature, T_g, determined by the tangent method from the dilatometric curve in Fig. 1 is ≈740 °C. A typical DTA trace measured at the heating rate of 5 K min^{-1} in Fig. 2 shows two exothermic peaks. The first occurs at ≈880 °C, corresponding to crystallization of apatite, and the second occurs at ≈1008 °C, corresponding to crystallization of wollastonite, as analysed by the X-ray diffraction (XRD). These results agree with those reported by Kokubo *et al*. [4].

Fig. 3 shows the DTA traces of the coarse glass particles measured at heating rates of 5, 7 10, and 15 K min^{-1}. Variations of crystallization peak temperature, T_P, and crystallization on-set temperature, T_0, as a function of heating rate, ϕ, are observed for the first exotherms. For the second exotherms, only T_P varies as a function of heating rate. The onset temperature of the second exotherms is constant at ≈974 °C, except at the heating rate of 15 K min^{-1} where T_0 is ≈986 °C. T_0 and T_P are listed in Table III.

Fig. 4 shows the corresponding Kissinger plot from which the slopes, $-E/R$, are calculated by least squares fitting of the data to a straight line. The calculated E represents the activation energy for combined crystal nucleation and growth because no prior nucleation heat treatment was made in this study. The activation energy for crystallization of the first exotherm (i.e. of apatite phase) is ≈514 kJ mol^{-1}, and that of the second exotherm, i.e. of wollastonite phase, is ≈374 kJ mol^{-1}.

The Avrami parameter, n, calculated from Equation 2 is close to 3 for apatite crystallization, and ≈2 for wollastonite crystallization. The n value indicates that the crystallization mechanism of apatite is bulk

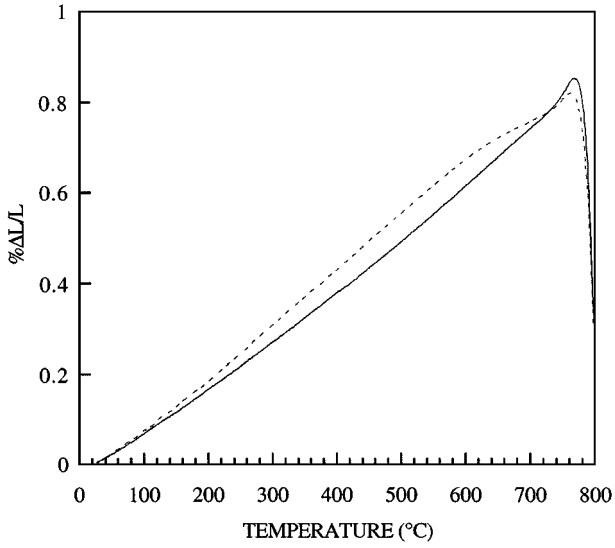

Figure 1 Dilatometric plots of the A–W glass. (- - -) As-quenched glass, (——) annealed at 750 °C for 1 h.

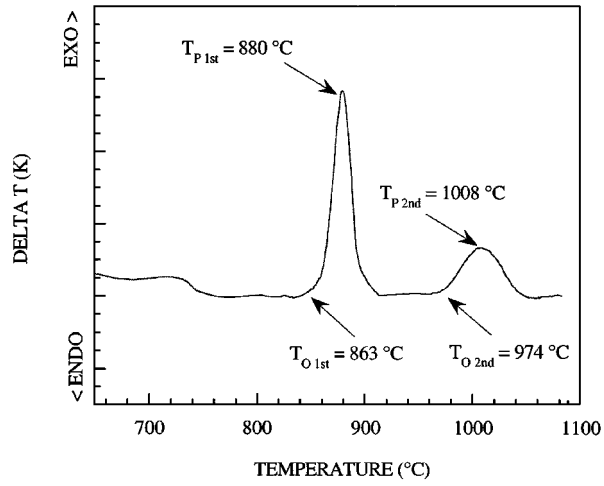

Figure 2 DTA trace of the glass with particle size of 1–2 mm measured at the heating rate of 5 K min^{-1}.

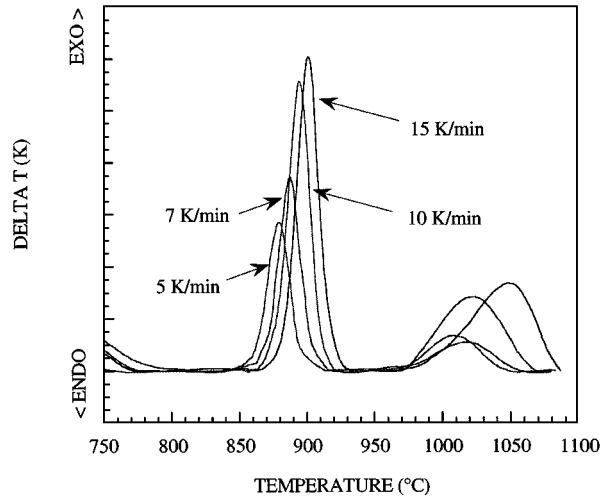

Figure 3 DTA traces of the glass with particle size of 1–2 mm measured at the heating rate of 5, 7, 10, and 15 K min^{-1}.

TABLE III DTA onset temperature and peak temperature as a function of heating rate

Heating rate (K min^{-1})	First exotherm		Second exotherm	
	T_0 (°C)	T_P (°C)[a]	T_0 (°C)	T_P (°C)[a]
5	863	880	974	1008
7	870	888	974	1018
10	874	896	974	1023
15	877	903	986	1047

[a]deviation of peak temperature is ±2 °C and ±4 °C for the first and second exotherm, respectively.

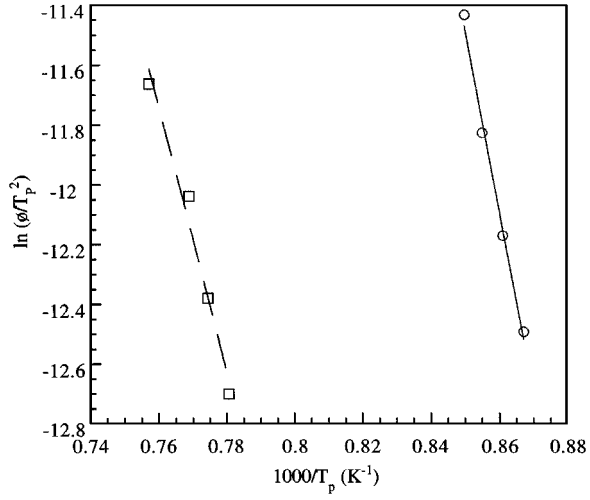

Figure 4 Kissinger analysis of glass with particle size 1–2 mm. (—○—) first exotherm, (—□—) second exotherm.

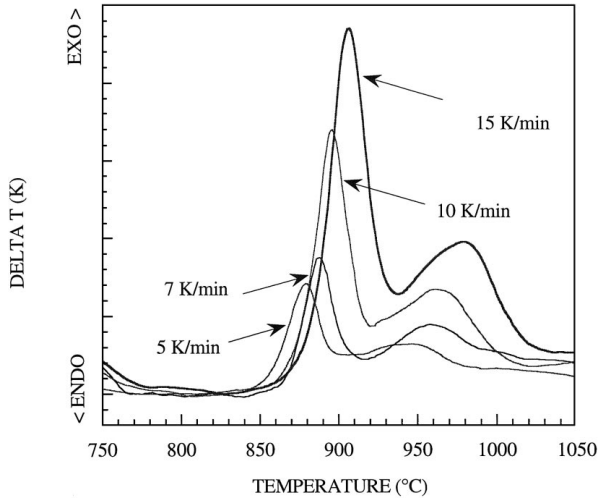

Figure 5 DTA traces of glass with particle size of 180–250 μm measured at the heating rate of 5, 7, 10, and 15 K min^{-1}.

crystallization, while that of wollastonite is surface crystallization (planar growth), in agreement with results reported by Illesova [11] for a similar bioglass system. Parameters used for the calculation and the resulting n values are shown in Table IV.

Activation energy for crystallization of the fine glass particles is evaluated from the DTA traces in Fig. 5. The T_P of the first exotherm measured at heating rates of 5, 7, and 10 K min^{-1} is identical to those of the coarse particles measured at corresponding heating rates (see

TABLE IV DTA peak temperature, FWHM, and kinetic parameters of glass with particle size 1–2 mm

	First exotherm $E = 514$ kJ mol^{-1}			Second exotherm $E = 374$ kJ mol^{-1}		
Heating rate (K min^{-1})	T_P (°C)	FWHM (K)	n	T_P (°C)	FWHM (K)	n
5	880	19	2.83	1008	45	2.03
7	888	20	2.72	1018	49	1.89
10	896	19	2.91	1023	54	1.73
15	903	20	2.80	1047	54	1.79

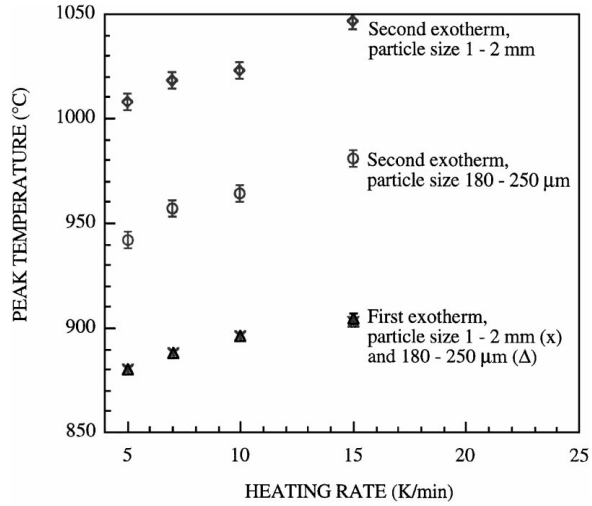

Figure 6 The first and second exothermic peak temperature of the glass with particle size 1–2 mm and 180–250 μm as a function of heating rate.

Fig. 3). T_P of the coarse and fine particles measured at the heating rate of 15 K min^{-1} are different by ≈4 K, but considering the experimental errors this difference appears negligible.

In the case of the second exotherm, a difference in T_P for the coarse and fine particles is observed. However, the trend of the peak shift as a function of heating rate is similar. Variations in T_P of the first and second exotherm as a function of heating rate of the coarse and fine glass-particle are compared in Fig. 6.

The activation energies for crystallization, E, of the fine particles obtained from the Kissinger plot in Fig. 7 is ≈482 kJ mol^{-1} and ≈346 kJ mol^{-1} for the first and the second exotherm, respectively. By taking the deviation of the peak temperature into consideration (see the note below Table III), the activation energies of the coarse and fine particles are 514 ± 57 and 482 ± 36 kJ mol^{-1} for the first exotherm, and 374 ± 34 and 346 ± 30 kJ mol^{-1} for the second exotherm, respectively. A statistical analysis using the student t-distribution [12] confirms that the difference in the activation energy between the coarse and the fine particles for the

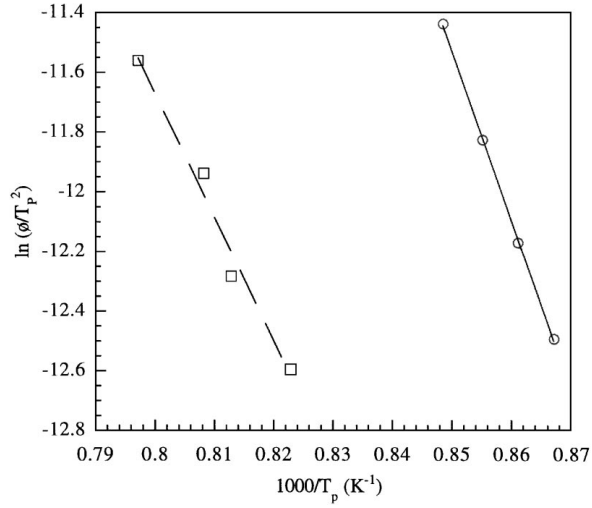

Figure 7 Kissinger analysis of glass with particle size 180–250 μm. (—○—) first exotherm, (—□—) second exotherm.

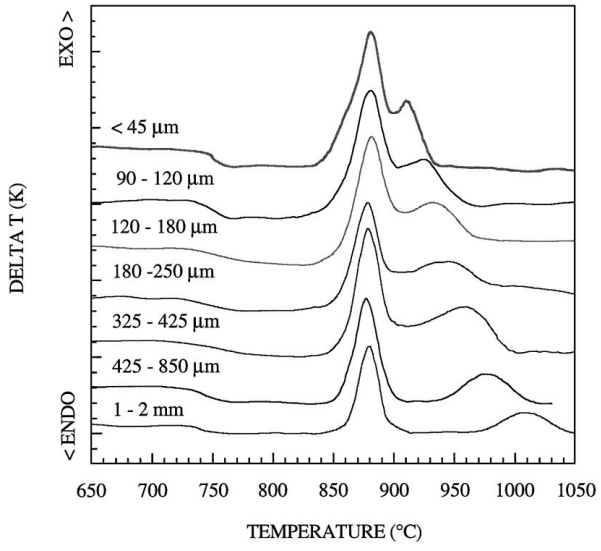

Figure 8 DTA traces of glass with particle size ranging from 1–2 mm to <45 μm measured at the heating rate of 5 K min^{-1}.

first exotherm is not significant within the 95% confidence interval. A similar analytical result is obtained for the second exotherm.

The independence of E on particle size of both exotherms, within the experimental errors, indicates that nuclei concentration is saturated and no nucleation rate is involved during the DTA measurements. This so-called site-saturation condition infers that the nucleation rate is negligible and that the evaluated activation energy is due to crystal growth [13]. As mentioned by Yinnon and Uhlmann [13], the crystal growth rate measured over a limited temperature range assumes Arrhenian temperature dependence. Therefore, the assumption that the overall reaction is an Arrhenian temperature dependence holds here.

The effect of glass particle size on DTA traces is shown in Fig. 8. No significant change in the peak position of the first exotherm is observed. T_P of the first exotherm occurs between 879 and 882 °C for the whole range of particle size. On the other hand, the peak position of the second exotherm clearly shifts to lower temperature as particle size decreases. T_P of the second exotherm decreases from 1008 °C to 912 °C with the decrease in particle size.

The decrease in T_P has been observed by other researchers in several glass systems and is assigned to an increase in the number of surface nuclei and surface areas with decrease in particle size [14, 15]. Thus, the strong dependence of the second exothermic peak temperature on particle size suggests that a surface crystallization mechanism dominates for the wollastonite phase.

The broad FWHM of the first exotherm as a function of particle size indicates that a surface crystallization mechanism is involved in the formation of apatite. However, the constant T_P of the first exotherm confirms that the increase in the number of surface nuclei has a minor effect on the crystallization mechanism of this phase, and suggests that the formation of apatite crystals is dominated by the bulk mechanism.

4. Conclusion

The crystallization kinetic parameters of the A–W glass obtained from the DTA indicate that the crystallization mechanism of the apatite phase was a three-dimensional bulk process with the reaction order, $n \approx 3$, while that of the wollastonite phase is a surface process (two-dimensional planar growth) with $n \approx 2$, for a bulk glass.

The activation energies for crystallization of the apatite phase for the coarse and fine particles are 514 ± 57 and 482 ± 36 kJ mol^{-1}, while that of wollastonite are 374 ± 34 and 346 ± 30 kJ mol^{-1}, respectively. There is no statistically significant effect of particle size on E for either phase. The independence of the activation energy on particle size from the DTA confirms the site-saturation condition (i.e. no nucleation rate involved during the measurements) and the activation energy is due to the crystal growth. Through these conditions, the overall crystallization reaction is assumed to exhibit an Arrhenian temperature dependence. These results, in turn, validate the approach used to determine the kinetics parameters by the non-isothermal method in this study.

The crystallization temperature of the wollastonite phase is strongly affected by the glass particle size. The peak position shifts to a lower temperature as the particle size becomes smaller. On the other hand, the crystallization temperature of the apatite phase is independent of the particle size. Overlap of the two exotherms is observed when the particle size is smaller than 120 μm.

References

1. T. NAKMURA, T. YAMAMURO, S. HIGASHI, T. KOKUBO and S. ITO, *J. Biomed. Mater. Res.* **19** (1985) 685.
2. T. KOKUBO, S. ITO, M. SHIGEMATSU, S. SAKKA and T. YAMAMURO, *J. Mater. Sci.* **20** (1985) 2001.
3. T. KOKUBO, S. ITO, S. SAKKA, M. SHIGEMATSU and T. YAMAMURO, *ibid.* **22** (1987) 4067.
4. T. KOKUBO, S. ITO, S. SAKKA and T. YAMAMURO, *ibid.* **21** (1986) 536.
5. L. L. HENCH, in "CRC Handbook of Bioactive Ceramics," Vol. 1, "Bioactive Glasses and Glass-Ceramics" (CRC Press, Boston, MA, 1990).
6. H. E. KISSINGER, *J. Res. Nat. Bur. Stand. (US)* **57** (1956) 217.
7. J. A. AUGIS and J. E. BENNETT, *J. Therm. Anal.* **13** (1978) 283.
8. A. MAROTTA, S. SAIELLO, F. BRANDA and A. BURI, *J. Mater. Sci.* **17** (1982) 105.
9. C. RAY and D. E. DAY, *J. Am. Ceram. Soc.* **73** (1990) 439.
10. A. MAROTTA, A. BURI and G. L. VALENTI, *J. Mater. Sci.* **13** (1978) 2483.
11. L. ILLESOVA, *J. Therm. Anal.* **44** (1995) 589.
12. R. E. WALPOLE, "Introduction to Statistics" (Macmillan, New York, 1990).
13. H. YINNON AND D. R. UHLMANN, *J. Non-Cryst. Solids* **54** (1983) 253.
14. K. MATUSITA and S. SAKKA, *ibid.* **38/39** (1980) 741.
15. A. MAROTTA, A. BURI, F. BRANDA and S. SAIELLO, lin "Advances in Ceramics," Vol. 4, "Nucleation and Crystallization in Glasses I" (The American Ceramic Society, Columbus, OH, 1982).

Received 18 December 1996
and accepted 23 July 1997